Electronic Supplementary Material (ESI) for Physical Chemistry Chemical Physics.

Supplementary Information

Low-lying, Diffuse Rydberg States of Polycyclic Aromatic Hydrocarbons (PAHs) and Cyclic Alkanes

E. Bohl, B. Mignolet, J.O. Johansson, F. Remacle and E. E. B. Campbell

1. Comparison of Functionals and Basis Sets

Different functionals and basis sets (Pople, split valence double zeta basis sets) were tested to determine which combination gave the best comparable results to literature values with a reasonable calculation time (not more than 24 hours for the excited state calculation). For these test runs, naphthalene was chosen because reliable experimental data on its Rydberg states were available from the literature.

The procedure to obtain the binding energies of the excited electronic states was as follows. First the ground state equilibrium geometry was determined using the chosen functional and basis set and imposing the relevant the symmetry point group. In the case of naphthalene the symmetry point group is D_{2h}. As a quick test of the reliability of the computational result, the calculated vertical ionisation energy (IE) was compared to the literature value, where the targeted variance was less than 5% of the value. The adiabatic IE was calculated only for a few functionals and basis sets as further verification of their accuracy. The computed IEs of the different functionals and basis sets are summarised in Table 1 for naphthalene.

Table 1. Comparison of computed IEs of naphthalene to experimental values at different levels of theory

Napthalene	Vertical I.E. / eV	Adiabatic I.E. / eV
Experimental values	8.14 ± 0.02 (1)	8.144 ± 0.001 (2)
Theory Level		
wB97XD/6-31(2+)+G(d,p)	7.99	--
M06HF/6-31(2+)+G(d,p)	8.51	--
B3LYP/6-31(2+)+G(d,p)	7.91	--
CAM-B3LYP/6-31(2+)+G(d,p)	8.05	7.94
wB97XD/6-31++G(d,p)	8.31	--
CAM-B3LYP/6-31(2+)+G(d,p)	8.05	7.94
CAM-B3LYP/6-31(2+)(2+)G(d,p)	8.05	7.94
CAM-B3LYP/6-31(3+)(3+)G(d,p)	8.05	--

All computed IEs are within 5% of the experimental value and below the experimental IE, except at the M06HF/6-31(2+)+G(d,p) and wB97XD/6-31++G(d,p) levels (Table 1). The M06HF functional neglects the self-exchange interactions at long range and uses the full Hartree-Fock exchange which may lead to a larger deviation. However, the wB97XD functional is long-range corrected and includes empirical dispersion, but the complementing basis set also needs to be large enough to enable a good approximation. In Table 1 the outcomes show that the basis set 6-31(2+)+G(d,p) has to be used with the wB97XD functional to obtain reasonably good results, whereas the 6-31++G(d,p) basis set is probably too small for the calculation of the IE of naphthalene. Altogether the best results are obtained with the CAM-B3LYP functional and a basis set of 6-31(2+)+G(d,p) at least (Table 1). Larger basis

sets with the CAM-B3LYP functional do not give a noticeable improvement in the IEs (Table 1).

The excited electronic states were then computed at the ground state equilibrium geometry using TD-DFT. Isocontours of the Dyson orbitals were inspected using the GaussView program(3) and by eye it was determined if the electron density has a symmetry similar to s, p or d orbitals. The binding energies of the states are obtained through the subtraction of the calculated excitation energy from the calculated vertical IE for each state. The resulting binding energies (BE) are compared to literature values as shown in Table 2.

Table 2. *Calculated binding energies of different excited states of naphthalene at the CAM-B3LYP/6-31(2+)+G(d,p) level compared to literature values.*

	LUMO + 1	LUMO + 2	LUMO+3	LUMO+4
Orbital shape	s	p_z	p_y	p_x
Calc. vertical IE / eV	8.05			
Calc. exc. energy / eV	5.55	5.91	5.94	5.94
Binding energy / eV	2.50	2.14	2.11	2.11
Lit. value of BE / eV	2.57 (4) 2.55±0.09 (5)	2.14 (4) 2.35±0.09 (5)		

This procedure was conducted on naphthalene for the different functionals and basis sets so that the binding energies could be compared. The obtained binding energies at the various theory levels are summarised graphically in Figure 1.

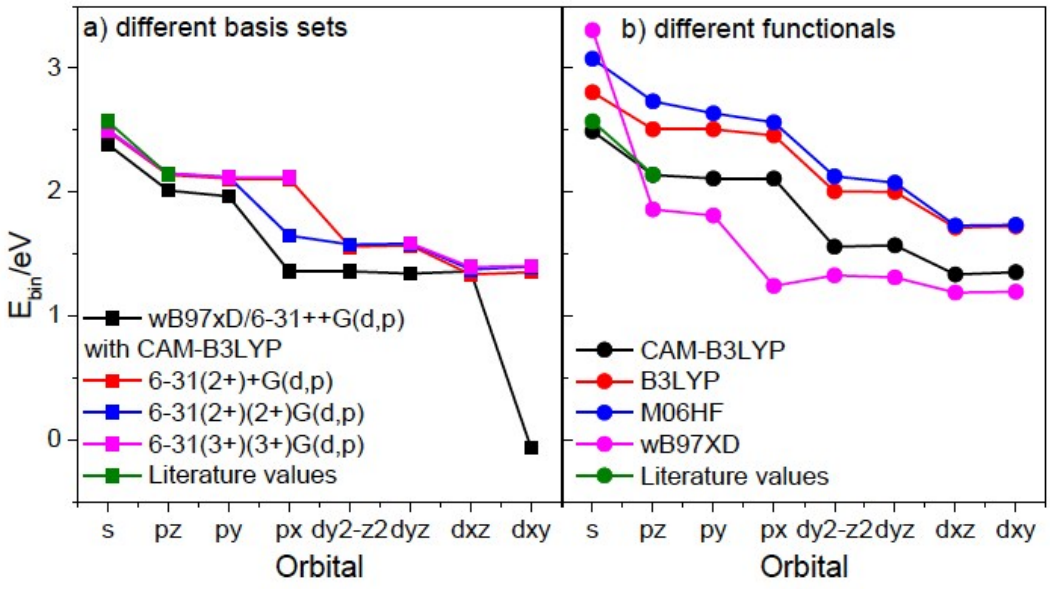

Figure 1. Comparison of the calculated binding energies for different excited states of naphthalene obtained using various a) basis sets and b) functionals (with 6-31(2+)+G(d,p) basis set). The computed results are also compared to literature values from (4).

On the basis of Fig. 1 the functional CAM-B3LYP with the basis set 6-31(2+)+G(d,p) was chosen as the most suitable level of theory. The larger basis sets (Figure 1a) increase the computational time, but do not provide a significant improvement on the binding energies because the basis set 6-31(2+)+G(d,p) already gives values close to the literature. The CAM-B3LYP functional shows the best agreement with the literature values for the binding energies of the s and p state, while the other functionals, which also include long range interactions like wB97XD as well as M06HF and B3LYP are farther off the literature values (Figure 1b).

2. Background Subtraction

The experimental coronene photoelectron spectra consist of three components: the Rydberg peak structure, a thermal background that has been reported previously for high laser intensities with 800nm excitation (6) and also explored in detail for fullerenes,(7) and an additional background signal for low kinetic energies, not observed from fullerenes, that may be attributed to photoionisation from excited valence states. Both the thermal background and the additional low kinetic energy

signal remain constant for different photoelectron emission angles. Fig. 2 shows the angle-integrated spectrum that was shown in Figs. 5 and 6 of the main paper. The black spectrum is the data as measured, after the POP inversion routine. The red spectrum has had the exponential thermal background signal subtracted with a fitted apparent electron temperature of 0.8 eV. The blue spectrum has had the additional background subtracted using a sigmoid function, $\propto (1 + \exp(-6(\varepsilon - 1.4))$. The blue curve was fitted with Gaussians to extract the Rydberg peak intensities as illustrated in Fig. 6 of the main paper. The same background subtraction was used for all emission angle segments.

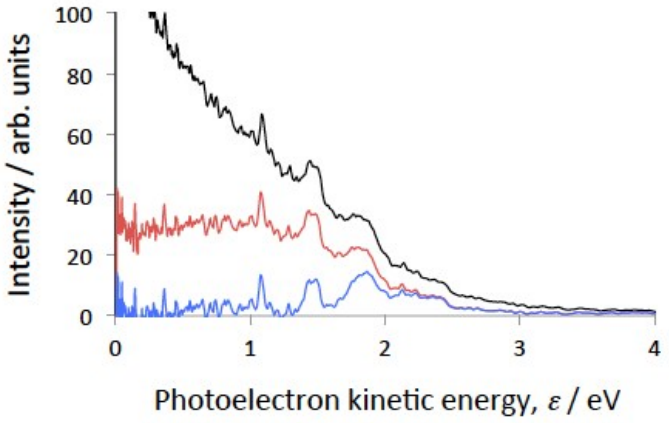

Fig. 2. Illustrating the background subtraction for the angle-integrated coronene spectrum. Black: as measured, red: with exponential thermal distribution subtracted, blue: with additional homogeneous background signal subtracted for low ε.

3. Key equations used for the computation of the photoionisation matrix elements, widths and angular distributions

A Dyson orbital(8-10) is defined as the overlap between two electronic states with a different number of electrons, the initial state with n electrons and the final state with n-1 electrons.

$$\phi_{IK}^{Dyson}(\mathbf{r}) = \sqrt{n}\int \Psi_I^{neut}(r_1 \ldots r_n)\Psi_K^{cat}(r_2 \ldots r_n)d\mathbf{r}_2 \ldots d\mathbf{r}_n \quad \backslash^* \text{ MERGEFORMAT (1.1)}$$

The Dyson orbital can be expressed in the basis of the molecular orbitals of the neutral φ_{κ}^{Neut}.

$$\phi_{IK}^{Dyson}(\mathbf{r}) = \sum_{\kappa=1} \lambda_{IJ}^{\kappa} \varphi_{\kappa}^{Neut}(\mathbf{r}) \quad \text{* MERGEFORMAT (1.2)}$$

with

$$\lambda_{IJ}^{\kappa} = \left\langle \Psi_K^{cat} \middle| \hat{p}_{\kappa} \Psi_I^{neut} \right\rangle \quad \text{* MERGEFORMAT (1.3)}$$

Where λ_{IJ}^{κ} is the overlap between the cationic wavefunction and the neutral wavefunction in which an electron has been removed from molecule orbital φ_{κ}^{Neut} by the operator $\hat{p}_{\kappa}$.

In the case of the PAHs, we investigated the photoionisation of the neutral excited states to their cationic ground state so Ψ_I^{neut} is the Ith excited state of the neutral and Ψ_K^{cat} is the ground state of the cation. Both the neutral excited states and cationic ground state are computed with the same functional and basis set.

As mentioned in the main text, a central quantity in the photoionisation study is the photoelectron matrix element(11), which is the dipolar coupling element between the wavefunction of a neutral excited state and the wavefunction of an ionised state.

$$D_{IK\varepsilon\Omega} = \left\langle \Psi_I^{neut} \middle| \mu \middle| \Psi_K^{cat}, \Psi_{\varepsilon,\Omega}^{elec} \right\rangle \quad \text{* MERGEFORMAT (1.4)}$$

This ionised state is defined as the antisymmetrised product of the *n*-1 electron wavefunction of the cationic state Ψ_K^{cat} with the wavefunction of the ionized electron, $\Psi_{\varepsilon,\Omega}^{elec}$, that is chosen to be a plane wave. The ionized electron has a given kinetic energy ε and an orientation Ω.

This n electron integral can be rewritten as the one electron dipole matrix element between the Dyson orbital, $\phi_{IK}^{Dyson}(\mathbf{r})$ and the wave function describing the ionising electron, $\Psi_{\varepsilon,\Omega}^{elec}(\mathbf{r})$.

$$D_{IK\varepsilon\Omega} = \left\langle \Psi_{\varepsilon,\Omega}^{elec} \middle| \mu \middle| \phi_{IK}^{Dyson} \right\rangle \qquad \text{* MERGEFORMAT (1.5)}$$

The one-photon ionisation width (12) of the Ith neutral excited state for a given electron kinetic energy ε is computed by integrating the square modulus of the photoelectron matrix element over all the photoelectron angular distributions Ω.

$$\Gamma_I(\varepsilon) = \rho(\varepsilon) f_0^2 \int \left| \left\langle \Psi_{\varepsilon,\Omega}^{elec} \middle| -\mathbf{E}\cdot\mu \middle| \phi_{IK}^{Dyson} \right\rangle \right|^2 d\Omega \quad \text{* MERGEFORMAT (1.6)}$$

Where $\rho(\varepsilon)$ is the density of states for the free electron, $\mathbf{E}$ is the electric field polarization vector and f_0 the field strength. The photoionisation widths depend on the field strength and orientation of the electric field.

The photoelectron angular distribution(10, 13, 14) (PAD) of the Ith neutral excited state for a given electron kinetic energy of ε is given by

$$\frac{d\sigma_I(\varepsilon)}{d\Omega} = \frac{8\pi e^2 \omega}{\varepsilon_0 c} \rho_\Omega(\varepsilon) \left| \left\langle \Psi_{\varepsilon,\Omega}^{elec} \middle| \mathbf{E}\cdot\mu \middle| \phi_{IK}^{Dyson} \right\rangle \right|^2 \quad \text{* MERGEFORMAT (1.7)}$$

Where $\rho_\Omega(\varepsilon)$ is the density of states of the free electron in the solid angle Ω.

For an oriented molecule both the photoionisation widths and PADs depend on the polarisation of the electric field. We performed the averaging over molecular orientation by randomly selecting 600 orientations of the electric field. Then for each orientation, we use Euler rotation to rotate the molecule and its PAD so that the electric field is oriented along a fixed direction and the molecules are randomly oriented. Then the 3D PADs are integrated over the azimuthal angle so that to obtain $I_I(\theta,\varepsilon)$ for each excited state Ψ_I^{neut}.

$$I_I(\theta,\varepsilon) = \frac{\sigma_{total}}{4\pi}\left(1+\beta(\varepsilon)P_2(\cos\theta)\right) \text{* MERGEFORMAT (1.8)}$$

Where θ is the polar angle, ε is the kinetic energy of the ionized electron, σ_{total} is the angle-integrated cross section and P_2 is the second order Legendre polynomial. We then compute the β parameter that depends on the photoelectron kinetic energy by fitting the $I_I(\theta,\varepsilon)$ curves.

References

1. Schmidt W. Photoelectron spectra of polynuclear aromatics. V. Correlations with ultraviolet

absorption spectra in the catacondensed series. J Chem Phys. 1977;66:828-45.
2. Corkum PB, Krausz F. Attosecond science. Nat Phys. 2007 Jun;3(6):381-7. PubMed PMID: ISI:000247344400011.
3. GaussView V, Roy Dennington, Todd A. Keith, and John M. Millam, Semichem Inc., Shawnee Mission, KS, 2016.
4. Kuthirummal N, Weber PM. Rydberg states: sensitive probes of molecular structure. Chem Phys Lett. 2003;378:647-53.
5. George GA, Morris GC. The intensity of absorption of napthalene from 30000 cm-1 to 53000 cm-1. J Mol Spectrosc. 1968;26:67-71.
6. Kjellberg M, Bulgakov AV, Goto M, Johansson O, Hansen K. Femtosecond electron spectroscopy of coronene, benzo[GHI]perylene, and anthracene. The Journal of Chemical Physics. 2010;133(7):074308.
7. Johansson JO, Campbell EEB. Probing excited electronic states and ionisation mechanisms of fullerenes. Chemical Society Reviews. 2013;42(13):5661-71.
8. Pickup BT. On the theory of fast photoionization processes. Chemical Physics. 1977;19(2):193-208.
9. Oana CM, Krylov AI. Dyson orbitals for ionization from the ground and electronically excited states within equation-of-motion coupled-cluster formalism: Theory, implementation, and examples. The Journal of Chemical Physics. 2007;127(23):234106-14.
10. Seabra GM, Kaplan IG, Zakrzewski VG, Ortiz JV. Electron propagator theory calculations of molecular photoionization cross sections: The first-row hydrides. The Journal of Chemical Physics. 2004 09/01/;121(9):4143-55.
11. Oana CM, Krylov AI. Cross sections and photoelectron angular distributions in photodetachment from negative ions using equation-of-motion coupled-cluster Dyson orbitals. J Chem Phys. 2009 Sep 28;131(12):124114. PubMed PMID: 19791859.
12. Mignolet B, Johansson JO, Campbell EEB, Remacle F. Probing Rapidly-Ionizing Super-Atom Molecular Orbitals in C60: A Computational and Femtosecond Photoelectron Spectroscopy Study. ChemPhysChem. 2013;14(14):3332-40.
13. Mignolet B, Levine RD, Remacle F. Localized electron dynamics in attosecond-pulse-excited molecular systems: Probing the time-dependent electron density by sudden photoionization. Physical Review A. 2012 11/30/;86(5):053429.
14. Deleuze M, Pickup BT, Delhalle J. Plane wave and orthogonalized plane wave many-body Green's function calculations of photoionization intensities. Molecular Physics. 1994 1994/11/01;83(4):655-86.